

## Article

# Prognostic Value of the Immunohistochemical Expression of Serine and Arginine-Rich Splicing Factor 1 (SRSF1) in Uveal Melanoma: A Clinico-Pathological and Immunohistochemical Study on a Series of 85 Cases

Giuseppe Broggi <sup>1</sup>, Luca Falzone <sup>2</sup>, Matteo Fallico <sup>3</sup>, Andrea Russo <sup>3</sup>, Michele Reibaldi <sup>3,4</sup>, Antonio Longo <sup>3</sup>,  
Teresio Avitabile <sup>3</sup>, Rocco De Pasquale <sup>5</sup>, Lidia Puzzo <sup>1</sup>, Pietro Valerio Foti <sup>6</sup>, Daniela Russo <sup>7</sup>,  
Rosa Maria Di Crescenzo <sup>7</sup>, Massimo Libra <sup>2</sup>, Stefania Staibano <sup>7,†</sup> and Rosario Caltabiano <sup>1,\*,†</sup>



**Citation:** Broggi, G.; Falzone, L.; Fallico, M.; Russo, A.; Reibaldi, M.; Longo, A.; Avitabile, T.; De Pasquale, R.; Puzzo, L.; Foti, P.V.; et al. Prognostic Value of the Immunohistochemical Expression of Serine and Arginine-Rich Splicing Factor 1 (SRSF1) in Uveal Melanoma: A Clinico-Pathological and Immunohistochemical Study on a Series of 85 Cases. *Appl. Sci.* **2021**, *11*, 7874. <https://doi.org/10.3390/app11177874>

Academic Editor: Francisco Arrebola

Received: 26 July 2021

Accepted: 25 August 2021

Published: 26 August 2021

**Publisher's Note:** MDPI stays neutral with regard to jurisdictional claims in published maps and institutional affiliations.



**Copyright:** © 2021 by the authors. Licensee MDPI, Basel, Switzerland. This article is an open access article distributed under the terms and conditions of the Creative Commons Attribution (CC BY) license (<https://creativecommons.org/licenses/by/4.0/>).

- <sup>1</sup> Department of Medical and Surgical Sciences and Advanced Technologies, G.F. Ingrassia, Anatomic Pathology, University of Catania, 95123 Catania, Italy; giuseppe.broggi@gmail.com (G.B.); lipuzzo@unict.it (L.P.)
  - <sup>2</sup> Laboratory of Experimental Oncology, Department of Biomedical and Biotechnological Sciences (BIOMETEC), University of Catania, 95123 Catania, Italy; luca.falzone@unict.it (L.F.); mlibra@unict.it (M.L.)
  - <sup>3</sup> Department of Ophthalmology, University of Catania, 95123 Catania, Italy; matteofallico@hotmail.com (M.F.); andrearusso2000@hotmail.com (A.R.); mreibaldi@libero.it (M.R.); antlongo@unict.it (A.L.); t.avitabile@unict.it (T.A.)
  - <sup>4</sup> Department of Surgical Sciences, Eye Clinic Section, University of Turin, 10126 Turin, Italy
  - <sup>5</sup> Department of General Surgery and Medical-Surgical Specialties, University of Catania, 95123 Catania, Italy; r.depasquale@unict.it
  - <sup>6</sup> Department of Medical Surgical Sciences and Advanced Technologies G.F. Ingrassia—Radiology I Unit, University Hospital Policlinico “G. Rodolico-San Marco”, 95123 Catania, Italy; pietrofoti@hotmail.com
  - <sup>7</sup> Department of Advanced Biomedical Sciences, Pathology Section, University of Naples Federico II, 80131 Naples, Italy; daniela.russo@unina.it (D.R.); rosamariadicrescenzo@gmail.com (R.M.D.C.); staibano@unina.it (S.S.)
- \* Correspondence: rosario.caltabiano@unict.it; Tel.: +39-(09)-53782021  
† These authors share co-senior authorship.

**Abstract:** Uveal melanoma (UM) is the most frequent primary ocular malignancy of adults; it exhibits an almost invariably poor prognosis with onset of liver metastases within 10–15 years after the diagnosis. Serine and arginine-rich splicing factor 1 (SRSF1) is an RNA-binding protein with proto-oncogene functions, including stimulation of angiogenesis, cell migration and cell growth; regarding the complex regulation of tumor angiogenesis, it has been suggested that SRSF1 regulates the alternative splicing of vascular endothelial growth factor- $\alpha$ , promoting the formation of its pro-angiogenic isoform. The immunohistochemical expression of SRSF1 on a series of 85 primary UMs, including 39 metastasizing and 46 non-metastasizing cases, was investigated; to clarify the potential pathogenetic role of SRSF1 in this tumor and its effect on angiogenesis, we correlated our immunohistochemical findings with the clinico-pathological features, the prognostic data and blood vascular microvessel density (MVD) findings of the cases from our series. Cases with higher immunohistochemical expression of SRSF1 also had higher MVD, higher metastatic potential and shorter metastasis-free survival; conversely, cases with lower SRSF1 immunorexpression showed lower MVD, lower metastatic risk and longer metastasis-free survival times. Our results suggested that SRSF1 has a negative prognostic role and a pro-angiogenic function in UM.

**Keywords:** uveal melanoma; SRSF1; prognostic factor; MVD; metastasis; melanoma

## 1. Introduction

Melanoma of the uveal tract is an uncommon malignancy, mainly affecting middle-aged adult patients, primarily arising from the choroid and less frequently from the ciliary bodies and iris [1–4]. Uveal melanoma (UM), despite representing the most common

primary intraocular malignant tumor of the adult age, is exceptionally unusual in the pediatric population in which it usually has congenital origin with poorer outcome and more frequent extraocular extension at the diagnosis [5]. Risk factors that have historically been reported to be involved in the development of this neoplasm include: Fitzpatrick phototypes I-II, type 1 neurofibromatosis (NF-1), oculo-dermal melanocytosis (Ota nevus), dysplastic nevus syndrome, and choroidal nevi [5–7]. Although UM typically tends to remain asymptomatic for years before the diagnosis, a sudden retinal detachment often represents the presenting symptom of the tumor [1–5]. UM is a slow-growing tumor with indolent biological behavior but consistently poor prognosis, characterized by the development of liver metastases within 10–15 years after the diagnosis in about 50% of cases [6–9]. In recent years, the search for genetic and epigenetic prognostic and/or predictive factors of therapeutic response has been one of the most studied topics in cancer research [10,11]; in this regard, loss-of-function mutations of BRCA1 associated protein-1 (BAP1), that have been observed in most metastasizing UM cases and correlated with the immunohistochemical loss of BAP-1 protein, represent one of the most reliable prognostic factors of this tumor [12–14]. Serine and arginine-rich splicing factor 1 (SRSF1) is part of the SR protein family, being involved in canonic and alternative pre-mRNA splicing and in the regulation of mRNA transcription [15,16]. Moreover, SRSF1 has also been reported as a proto-oncogene positively involved in tumor angiogenesis by regulating the alternative splicing of vascular endothelial growth factor- $\alpha$  (VEGFA) [17–21]. In this regard, it has been suggested that SRSF1 tends to promote the formation of the pro-angiogenic isoform of VEGFA, instead of the anti-angiogenic one [17–21]. Consistent with its stimulatory role on tumor angiogenesis, SRSF1 has been found overexpressed in several human neoplasms, including prostate, brain, breast, colorectal, liver, pleural and lung tumors [20,22–27]; however, to the best of our knowledge, no data on the role of this protein in UM are present in literature to date.

We herein investigated the immunohistochemical expression of SRSF1 on a series of 85 cases of primary UMs and correlated it with clinico-pathological features and prognostic data of the cases from our cohort; moreover, in order to further confirm the pro-angiogenic role of SRSF1, we performed a correlation between its immunohistochemical expression and blood vascular microvessel density (MVD) in tumor tissue.

## 2. Materials and Methods

Histologic specimens of 85 primary UMs, surgically enucleated at the Ophthalmologic Clinics of the University of Catania and of the University of Naples “Federico II” from October 2009 to October 2019, were retrospectively collected. The corresponding clinico-pathologic data were retrieved from the original pathologic reports. For all the patients from our cohort, the enucleation was the only therapeutic option, as they were not eligible for plaque brachytherapy or proton-beam radiotherapy. The present research complied with the Helsinki Declaration, and all experiments were approved by the local Ethics Committee, Comitato Etico Catania 1, University of Catania (ID: 003186-24). Of each case, representative paraffin-blocks were retrieved from the Pathology archives of the Department G.F. Ingrassia, University of Catania, and of the Department of Advanced Biomedical Sciences, University of Naples “Federico II”. We adopted the previously reported [5] criteria of exclusion to select the cases. Tissue samples were evaluated separately by three pathologists (G.B., L.P. and R.C.), with no awareness of the clinico-prognostic data of the patients.

The study included 39 metastasizing UMs and 46 non-metastasizing UMs. We collected the following clinical data: (i) tumor largest diameter and anatomic location, both evaluated by ophthalmoscopy and A- and B-scan ultrasound exams; (ii) metastatic spread, detected by liver ultrasound exams and whole body computed tomography (WBCT).

### 2.1. MVD Count and Immunohistochemical Analyses

MVD was counted by three pathologists (G.B., L.P. and R.C.), by identifying vascular hotspots on immunohistochemical slides from each UM case stained with CD31, as previ-

ously described [20,26]. MVD was assessed as high-MVD if higher than the median value, and as low-MVD if lower than the median value.

Immunohistochemical analyses were performed as previously described [26–28]; briefly, standard and appropriate deparaffinization and pre-treatments were performed; subsequently, the sections were incubated for 30 min at 37 °C with mouse monoclonal anti-SRSF1 antibody (sc-33652; working dilution 1:50; Santa Cruz Biotechnology; Dallas, TX, USA) and with mouse monoclonal anti-CD31 antibody (JC70A; working dilution 1:40; DAKO, Glostrup, Denmark). The presence of brown chromogen within tumor nuclei was interpreted as positive SRSF1 immunohistochemical staining; non-pathologic gallbladder mucosa was used as positive control, while negative control slides were obtained by incubating them with phosphate-buffered saline instead of the primary antibody. UM cases stained with SRSF1 were semi-quantitatively analyzed, as previously described [26–28]: the Intensity of Staining (IS) was evaluated on a 0–3 scale (mild, moderate and strong), while the Extent Score (ES) (the percentage of positive cells) on a 0–4 scale (<5%; 5–30%; 31–50%; 51–75%; >75%). We obtained the Immunoreactivity Score (IRS) by multiplying IS and ES, and considered the immunohistochemical expression of SRSF1 as low if IRS was  $\leq 6$  (L-IRS), and as high if IRS  $> 6$  (H-IRS).

## 2.2. Statistical Analysis

For determination of high and low SRSF1 and MDV expression values, the better discriminant value was determined by the Youden index, assessed by ROC curve. The rates of high and low levels of SRSF1 and MDV expression in melanoma of patients with and without metastasis were non parametrically compared by chi-square tests. Agreement among observers was tested by Cohen's K. Moreover, we performed univariate and multivariate analyses, based on a Cox proportional hazards regression model (metastasis-free time as the outcome); this model included: (i) age, (ii) gender, (iii) tumor location (choroid vs ciliary body), (iv) temporal or nasal anatomic site, (v) cell subtype (epithelioid vs spindle cell vs mixed), (vi) echography parameters (height and largest diameter), (vii) immunorexpression (low and high) of SRSF1 and MVD. If a predictor had a  $p$  value  $< 0.15$  (cut off) in the univariate analysis, it was included in the multivariate one. Survival analysis according to SRSF1 and MVD expression levels (high and low) was performed by Kaplan–Meyer test; survival rates were compared by log-rank (Mantel–Cox) test.  $p$  values  $< 0.05$  were considered as statistically significant.

## 3. Results

### 3.1. Clinico-Pathologic Features of UMs

Tables 1 and 2 summarize the clinico-pathologic features of UMs from our series.

The study included 85 patients, of which 44 were males and 41 were females (median age: 67 years; age range 29–85). An exclusive choroidal localization and a simultaneous involvement of the choroid and ciliary bodies were found in 64 and 21 UMs, respectively. Three cases showed extrascleral invasion. Histologically, 20 cases exhibited an epithelioid morphology, 25 a spindle cell morphology, while 40 cases were diagnosed as mixed-type. Thirty-nine patients showed liver metastases. Follow-up times ranged from 8 to 138 months (median value: 58 months).

**Table 1.** Tumour parameters, metastasis-free time, follow-up, SRSF1 and MDV in primary uveal melanoma without metastasis.

| Sex | Age (Years) | Location | Thickness (mm) | Largest Diameter (mm) | Cell Type | PT Stage | MFS (Months) | Follow-Up (Months) | SRSF1 |    |     |                  | MVD (n/mm <sup>2</sup> ) |   |
|-----|-------------|----------|----------------|-----------------------|-----------|----------|--------------|--------------------|-------|----|-----|------------------|--------------------------|---|
|     |             |          |                |                       |           |          |              |                    | IS    | ES | IRS | L (<3)<br>H (≥3) | L (<43)<br>H (≥43)       |   |
| F   | 29          | ch       | 14.2           | 16.2                  | mixed     | pT2a     | 169          | 169                | 0     | 0  | 0   | L                | 18                       | L |
| F   | 83          | ch/cb    | 14.84          | 16.8                  | mixed     | pT2b     | 123 (+)      | 123 (+)            | 1     | 1  | 1   | L                | 24                       | L |
| F   | 55          | ch       | 9.8            | 13.9                  | spindle   | pT2a     | 153          | 153                | 0     | 0  | 0   | L                | 21                       | L |
| F   | 30          | ch/cb    | 12.05          | 9.2                   | spindle   | pT2b     | 153          | 153                | 0     | 0  | 0   | L                | 16                       | L |
| M   | 74          | ch/cb    | 10.04          | 16.1                  | spindle   | pT2b     | 152          | 152                | 1     | 1  | 1   | L                | 26                       | L |
| M   | 64          | ch       | 7.7            | 11.5                  | spindle   | pT1a     | 143          | 143                | 0     | 0  | 0   | L                | 13                       | L |
| F   | 36          | ch       | 5.81           | 12.7                  | spindle   | pT1a     | 140          | 140                | 2     | 2  | 4   | H                | 20                       | L |
| F   | 59          | ch       | 8.4            | 16.7                  | mixed     | pT2a     | 139          | 139                | 0     | 0  | 0   | L                | 19                       | L |
| M   | 36          | ch       | 6.47           | 9.8                   | mixed     | pT1a     | 139          | 139                | 1     | 2  | 2   | L                | 32                       | L |
| M   | 84          | ch/cb    | 11.9           | 14.8                  | mixed     | pT2b     | 106 (+)      | 106 (+)            | 1     | 1  | 1   | L                | 25                       | L |
| F   | 67          | ch       | 10.42          | 13.2                  | mixed     | pT3a     | 136          | 136                | 0     | 0  | 0   | L                | 24                       | L |
| M   | 73          | ch       | 9.7            | 11.3                  | mixed     | pT2a     | 102 (+)      | 102 (+)            | 0     | 0  | 0   | L                | 17                       | L |
| F   | 45          | ch       | 13.7           | 10.2                  | mixed     | pT2a     | 127          | 127                | 2     | 2  | 4   | H                | 33                       | L |
| M   | 58          | ch       | 13.1           | 14.3                  | mixed     | pT2a     | 127          | 127                | 0     | 0  | 0   | L                | 29                       | L |
| M   | 63          | ch       | 3.3            | 11.7                  | spindle   | pT2a     | 116          | 116                | 0     | 0  | 0   | L                | 42                       | L |
| M   | 54          | ch       | 6.32           | 10                    | spindle   | pT2a     | 114          | 114                | 0     | 0  | 0   | L                | 29                       | L |
| M   | 83          | ch       | 10.62          | 9.4                   | epit      | pT3a     | 72 (+)       | 72 (+)             | 0     | 0  | 0   | L                | 44                       | H |
| F   | 71          | ch       | 3.68           | 6.4                   | epit      | pT1a     | 102          | 102                | 1     | 2  | 2   | L                | 33                       | L |
| M   | 55          | ch/cb    | 7.5            | 8.9                   | epit      | pT2b     | 92           | 92                 | 0     | 0  | 0   | L                | 16                       | L |
| M   | 52          | ch       | 9.2            | 12.1                  | spindle   | pT2b     | 91           | 91                 | 0     | 0  | 0   | L                | 14                       | L |
| M   | 46          | ch       | 8.76           | 11.3                  | spindle   | pT2a     | 85           | 85                 | 1     | 1  | 1   | L                | 24                       | L |
| F   | 76          | ch       | 8.02           | 10.7                  | mixed     | pT1a     | 79           | 79                 | 2     | 2  | 4   | H                | 18                       | L |
| F   | 63          | ch       | 10.3           | 13.7                  | mixed     | pT2a     | 73           | 73                 | 2     | 1  | 2   | L                | 26                       | L |
| F   | 41          | ch       | 5.85           | 10.3                  | mixed     | pT1a     | 73           | 73                 | 0     | 0  | 0   | L                | 35                       | L |
| F   | 55          | ch       | 3.2            | 7.6                   | mixed     | pT2a     | 55           | 55                 | 0     | 0  | 0   | L                | 28                       | L |
| M   | 68          | ch/cb    | 10.1           | 10.1                  | epit      | pT1b     | 55           | 55                 | 1     | 4  | 4   | H                | 37                       | L |
| M   | 74          | ch/cb    | 14.45          | 17.5                  | epit      | pT4b     | 49           | 49                 | 0     | 0  | 0   | L                | 45                       | H |
| M   | 70          | ch/cb    | 16.27          | 20.8                  | spindle   | pT4b     | 43           | 43                 | 1     | 1  | 1   | L                | 31                       | L |
| M   | 66          | ch       | 9.2            | 14.1                  | mixed     | pT3a     | 43           | 43                 | 1     | 4  | 4   | H                | 20                       | L |
| M   | 64          | ch       | 9.3            | 15.2                  | mixed     | pT2a     | 29           | 29                 | 0     | 0  | 0   | L                | 15                       | L |
| M   | 71          | ch       | 13.93          | 10.2                  | mixed     | pT2a     | 25           | 25                 | 0     | 0  | 0   | L                | 22                       | L |
| M   | 19          | ch       | 9.77           | 14.8                  | mixed     | pT2a     | 20           | 20                 | 1     | 1  | 1   | L                | 25                       | L |
| M   | 73          | ch       | 15.89          | 18                    | mixed     | pT2a     | 19           | 19                 | 0     | 0  | 0   | L                | 39                       | L |
| F   | 80          | ch       | 14.61          | 14.3                  | epit      | pT1b     | 15           | 15                 | 2     | 2  | 4   | H                | 18                       | L |
| F   | 81          | ch/cb    | 8.9            | 10.7                  | mixed     | pT2a     | 15           | 15                 | 1     | 1  | 1   | L                | 51                       | H |
| F   | 78          | ch       | 12             | 12                    | mixed     | pT3a     | 10           | 10                 | 1     | 1  | 1   | L                | 31                       | L |
| M   | 52          | ch       | 12             | 12                    | spindle   | pT3a     | 22           | 22                 | 0     | 0  | 0   | L                | 18                       | L |
| M   | 59          | ch       | 16             | 16                    | spindle   | pT4a     | 24           | 24                 | 0     | 0  | 0   | L                | 40                       | L |
| M   | 48          | ch       | 5              | 9                     | mixed     | pT1a     | 24           | 24                 | 0     | 0  | 0   | L                | 23                       | L |
| F   | 75          | ch       | 5              | 10                    | spindle   | pT2a     | 31           | 31                 | 0     | 0  | 0   | L                | 24                       | L |
| F   | 58          | ch       | 8              | 21                    | spindle   | pT4a     | 32           | 32                 | 0     | 0  | 0   | L                | 45                       | H |
| M   | 54          | ch       | 8              | 13                    | spindle   | pT3a     | 36           | 36                 | 0     | 0  | 0   | L                | 71                       | H |
| M   | 73          | ch       | 12             | 14                    | spindle   | pT3b     | 36           | 36                 | 1     | 1  | 1   | L                | 59                       | H |
| F   | 48          | ch       | 12             | 16                    | epit      | pT3b     | 37           | 37                 | 1     | 1  | 1   | L                | 28                       | L |
| F   | 70          | ch/cb    | 15             | 20                    | mixed     | pT4b     | 70           | 70                 | 0     | 0  | 0   | L                | 40                       | L |
| F   | 74          | ch       | 10             | 16                    | mixed     | pT3a     | 136          | 136                | 0     | 0  | 0   | L                | 37                       | L |

Abbreviations: MFS, metastasis-free survival; ch, choroid; cb, ciliary body; epit, epithelioid. (+) death

**Table 2.** Tumour parameters, metastasis-free time, follow-up, SRSF1 and MDV in primary uveal melanoma with metastasis.

| Sex | Age (Years) | Location | Thickness (mm) | Largest Diameter (mm) | Cell Type | PT Stage | MFS (Months) | Follow-Up (Months) | SRSF1 |    |     |                  | MVD (n/mm <sup>2</sup> ) |   |
|-----|-------------|----------|----------------|-----------------------|-----------|----------|--------------|--------------------|-------|----|-----|------------------|--------------------------|---|
|     |             |          |                |                       |           |          |              |                    | IS    | ES | IRS | L (<3)<br>H (≥3) | L (<43)<br>H (≥43)       |   |
| F   | 58          | ch       | 6.04           | 17.8                  | mixed     | pT2a     | 63           | 64 (+)             | 2     | 3  | 6   | H                | 39                       | L |
| M   | 69          | ch       | 7.21           | 15.8                  | mixed     | pT2a     | 54           | 81 (+)             | 1     | 4  | 4   | H                | 69                       | H |
| F   | 75          | ch/cb    | 15.5           | 15.3                  | mixed     | pT3b     | 44           | 62 (+)             | 3     | 3  | 9   | H                | 40                       | L |
| F   | 50          | ch       | 7.36           | 15.6                  | epit      | pT2a     | 41           | 111                | 0     | 0  | 0   | L                | 56                       | H |
| M   | 62          | ch       | 13.68          | 16                    | mixed     | pT3a     | 38           | 51 (+)             | 2     | 4  | 8   | H                | 63                       | H |
| F   | 51          | ch/cb    | 11.4           | 18.5                  | mixed     | pT3b     | 38           | 92                 | 2     | 2  | 4   | H                | 35                       | L |
| M   | 71          | ch       | 13.14          | 17.1                  | epit      | pT3a     | 33           | 34 (+)             | 0     | 0  | 0   | L                | 58                       | H |
| M   | 76          | ch/cb    | 11.6           | 6.5                   | mixed     | pT1a     | 31           | 70                 | 2     | 3  | 6   | H                | 54                       | H |
| M   | 72          | ch       | 10.3           | 15.4                  | mixed     | pT3b     | 27           | 35 (+)             | 3     | 2  | 6   | H                | 70                       | H |
| F   | 85          | ch/cb    | 7.3            | 14.7                  | spindle   | pT2d *   | 26           | 49 (+)             | 2     | 2  | 4   | H                | 45                       | H |
| M   | 73          | ch       | 5.73           | 11.7                  | epit      | pT2a     | 26           | 42 (+)             | 3     | 3  | 9   | H                | 56                       | H |
| F   | 51          | ch       | 9.42           | 19                    | mixed     | pT3a     | 25           | 71                 | 2     | 3  | 6   | H                | 12                       | L |
| F   | 84          | ch       | 11.7           | 17.4                  | mixed     | pT3a     | 76           | 78 (+)             | 3     | 3  | 9   | H                | 28                       | L |
| M   | 73          | ch       | 9.24           | 17.7                  | epit      | pT2a     | 103          | 112 (+)            | 2     | 4  | 8   | L                | 76                       | H |
| F   | 74          | ch       | 5.7            | 12.1                  | spindle   | pT2a     | 24           | 37 (+)             | 2     | 2  | 4   | H                | 45                       | H |
| F   | 67          | ch       | 3.49           | 20                    | mixed     | pT4a     | 24           | 31 (+)             | 3     | 3  | 9   | H                | 55                       | H |
| M   | 74          | ch       | 11.35          | 10.5                  | epit      | pT3a     | 19           | 78                 | 2     | 3  | 6   | H                | 69                       | H |
| M   | 82          | ch       | 9.7            | 11                    | epit      | pT2a     | 19           | 42 (+)             | 2     | 2  | 4   | H                | 78                       | H |
| F   | 72          | ch       | 6.7            | 15.2                  | epit      | pT2a     | 14           | 28 (+)             | 3     | 3  | 9   | H                | 72                       | H |
| M   | 76          | ch       | 13.7           | 17.1                  | mixed     | pT2a     | 14           | 101                | 2     | 4  | 8   | H                | 64                       | H |
| M   | 79          | ch       | 13.91          | 16.1                  | epit      | pT3b     | 13           | 79                 | 2     | 2  | 4   | H                | 45                       | H |
| F   | 66          | ch/cb    | 8.95           | 12.5                  | mixed     | pT2b     | 12           | 37 (+)             | 3     | 3  | 9   | H                | 58                       | H |
| F   | 74          | ch       | 8.6            | 10.2                  | mixed     | pT4b     | 23           | 43                 | 2     | 3  | 6   | H                | 69                       | H |
| F   | 60          | ch       | 8.25           | 16.5                  | epit      | pT2a     | 11           | 37 (+)             | 2     | 2  | 4   | H                | 74                       | H |
| F   | 57          | ch/cb    | 13.6           | 19                    | epit      | pT2b     | 6            | 86                 | 2     | 3  | 6   | H                | 46                       | H |
| M   | 72          | ch/cb    | 13.3           | 15.4                  | mixed     | pT3b     | 0            | 82                 | 3     | 3  | 9   | L                | 58                       | H |
| M   | 78          | ch       | 16.58          | 16.6                  | epit      | pT2b     | 2            | 3 (+)              | 2     | 3  | 6   | H                | 44                       | H |
| F   | 60          | ch       | 3.2            | 13.5                  | spindle   | pT3a     | 44           | 44                 | 2     | 2  | 4   | H                | 11                       | L |
| F   | 66          | ch       | 15             | 18                    | spindle   | pT2a     | 48           | 48                 | 3     | 3  | 9   | H                | 66                       | H |
| F   | 50          | ch/cb    | 9              | 12                    | epit      | pT4b     | 49           | 49                 | 2     | 4  | 8   | H                | 24                       | L |
| F   | 70          | ch/cb    | 23             | 23                    | spindle   | pT2b     | 58           | 58                 | 2     | 4  | 8   | H                | 15                       | L |
| F   | 81          | ch       | 15             | 18                    | mixed     | pT4a     | 6            | 12 (+)             | 3     | 3  | 9   | H                | 28                       | L |
| M   | 60          | ch/cb    | 6              | 6                     | spindle   | pT4d *   | 12           | 17 (+)             | 3     | 3  | 9   | H                | 44                       | H |
| F   | 73          | ch/cb    | 15             | 15                    | epit      | pT3d *   | 14           | 18 (+)             | 3     | 3  | 9   | H                | 33                       | L |
| M   | 59          | ch       | 12             | 11                    | mixed     | pT4a     | 12           | 18 (+)             | 3     | 3  | 9   | H                | 34                       | L |
| M   | 68          | ch       | 9              | 15                    | spindle   | pT3b     | 18           | 24 (+)             | 2     | 1  | 2   | L                | 54                       | H |
| M   | 56          | ch       | 11             | 9                     | spindle   | pT3a     | 24           | 36 (+)             | 2     | 4  | 8   | H                | 25                       | L |
| M   | 82          | ch       | 15             | 18                    | mixed     | pT4a     | 48           | 60 (+)             | 2     | 4  | 8   | H                | 23                       | L |
| M   | 66          | ch       | 3.2            | 13.5                  | spindle   | pT2a     | 80           | 111 (+)            | 2     | 2  | 4   | H                | 58                       | H |

Abbreviations: MFS, metastasis-free survival; ch, choroid; cb, ciliary body; epit, epithelioid. \* extrascleral extension. (+) death.

The cohort of 46 non-metastasizing cases included 25 males and 21 females with ages ranging from 19 to 84 months (median: 64 years). Among the 39 metastasizing UMs, 19 were males and 20 were females, with ages ranging from 50 to 85 years (median: 71 years). As a result of disease progression, 25 out of 39 metastatic patients died during the follow-up period. No significant differences were observed in median age, melanoma anatomic location (choroid or choroid and ciliary body), melanoma thickness, histologic

subtype, extrascleral extension and pathologic T stage between metastasizing and non-metastasizing cases; patients with metastatic spread exhibited tumors with greater median largest diameter (15.4 mm versus 12.4 mm,  $p = 0.009$ ), higher median SRSF1 expression (6 versus 0,  $p < 0.001$ ), higher median MVD levels (54 versus 26,  $p < 0.001$ ) and shorter median metastasis-free survival (25 months versus 73 months,  $p < 0.001$ ) (Table 3).

**Table 3.** Median (range) of demographics, tumour parameters, metastasis-free time, follow-up, SRSF1 expression and MVD in primary uveal melanoma without and with systemic metastasis.

|                                                    | Sex<br>m-f | Age<br>(Years) | Location          | Thickness          | Largest<br>Diameter | Cell Type                            | Pathological<br>T stage                                                                                            | MFS<br>(Months) | Follow-Up<br>(Months)      | SRSF1      | MVD<br>(n/mm <sup>2</sup> ) |
|----------------------------------------------------|------------|----------------|-------------------|--------------------|---------------------|--------------------------------------|--------------------------------------------------------------------------------------------------------------------|-----------------|----------------------------|------------|-----------------------------|
| All<br>(n = 85)                                    | 44-41      | 67<br>(29-85)  | ch 64<br>ch/cb 21 | 10.0<br>(3.2-16.3) | 14.3<br>(6.4-20.8)  | Epit: 20<br>Spindle: 25<br>Mixed: 40 | pT1a: 15<br>pT1b: 4<br>pT2a: 44<br>pT2b: 16<br>pT2d: 1 ee<br>pT3a: 20<br>pT3b: 10<br>pT4a: 6<br>pT4b: 8<br>pT4d: 1 | 41<br>(0-138)   | 58<br>(8-138)              | 2<br>(0-9) | 34<br>(11-78)               |
| Metastasis<br>free<br>(n=46)                       | 25-21      | 64<br>(19-84)  | ch 36<br>ch/cb 10 | 9.9<br>(3.2-16.2)  | 12.9<br>(6.4-21)    | Epit: 7<br>Spindle: 16<br>Mixed: 23  | pT1a: 7<br>pT1b: 2<br>pT2a: 17<br>pT2b: 6<br>pT3a: 7<br>pT3b: 2<br>pT4a: 2<br>pT4b: 3                              | 73<br>(10-169)  | 73<br>(10-169)<br>4 deaths | 0<br>(0-8) | 26<br>(13-71)               |
| Metastasis<br>(n=39)                               | 19-20      | 71<br>(50-85)  | ch 28<br>ch/cb 11 | 10.3<br>(3.2-23)   | 15.4<br>(6-23)      | Epit: 13<br>Spindle: 9<br>Mixed: 17  | pT1a: 8<br>pT1b: 2<br>pT2a: 28<br>pT2b: 10<br>pT2d: 1 ee<br>pT3a: 13<br>pT3b: 8<br>pT4a: 4<br>pT4b: 5<br>pT4d: 1   | 25<br>(0-109)   | 49<br>(1-112)<br>25 deaths | 6<br>(0-9) | 54<br>(11-78)               |
| <i>p</i><br>(metastasis<br>free vs.<br>metastasis) | 0.666 °    | 0.099 *        | 0.615 °           | 0.932 *            | 0.009 *             | 0.493 *                              | 0.271 *                                                                                                            | <0.001 *        | 0.031 *                    | <0.001 *   | <0.001 *                    |

Epit, epithelioid; \* Kolmogorov-Smirnov test; ° Fisher's exact test.

### 3.2. Immunohistochemical Expression of SRSF1 and MVD Count in UMs

Among the whole cohort of 85 UMs, the median SRSF1 value was 2. The better discriminant SRSF1 value as assessed by the Youden index of the ROC curve was 3. SRSF1 expression was high ( $\geq 3$ ) in 41 and low ( $< 3$ ) in 44 UMs (Figure 1A,B).

Among 46 primary non-metastatic UMs, SRSF1 L-IRS was found in 39/46 cases (84.8%), while SRSF1 H-IRS was observed in the remaining 7/46 cases (15.2%) (Fisher's exact test,  $p < 0.001$ , Table 4). In terms of primary metastatic UMs, 5 out of 39 (12.8%) exhibited SRSF1 L-IRS, while 34 out of 39 (87.2%) exhibited SRSF1 H-IRS (Fisher's exact test,  $p < 0.001$ , Table 4). Among the whole cohort of 85 UMs, MVD levels ranged from 11 to 78 (median MVD: 34). The better discriminant SRSF1 value as assessed by the Youden index of the ROC curve was 43. High and low MVD levels were observed in 32 and 53 UMs, respectively. A total of 40/46 (87%) non-metastatic cases exhibited low MVD, while 6/46 (13%) exhibited high MVD (Fisher's exact test,  $p < 0.001$ , Table 4). Moreover, high and low MVD levels were found in 26/39 (66.7%) and 13/39 (33.3%) metastasizing cases, respectively (Fisher's exact test,  $p < 0.001$ , Table 4). Statistical analyses showed that the following factors were related to the metastatic spread at univariate analysis on a Cox proportional hazards regression model: (i) age ( $p = 0.011$ ), (ii) diameter ( $p = 0.040$ ), (iii) epithelioid cell type ( $p = 0.017$ ), (iv) pT stage ( $p = 0.023$ ), (v) SRSF1 ( $p < 0.001$ ), (vi) MVD levels ( $p < 0.001$ ). At multivariate analysis, epithelioid cell type ( $p = 0.014$ ), pT stage ( $p = 0.001$ ), SRSF1 ( $p < 0.001$ ), and MVD ( $p < 0.001$ ) were significant. We observed no

significant correlations between histologic subtype, SRSF1 immunoeexpression (Spearman's rho  $p = 0.115$ ), and MVD (Spearman's rho  $p = 0.087$ ). A significant correlation was found between SRSF1 IRS and MVD (Spearman's rho  $r = 0.322$ ,  $p = 0.007$ ).

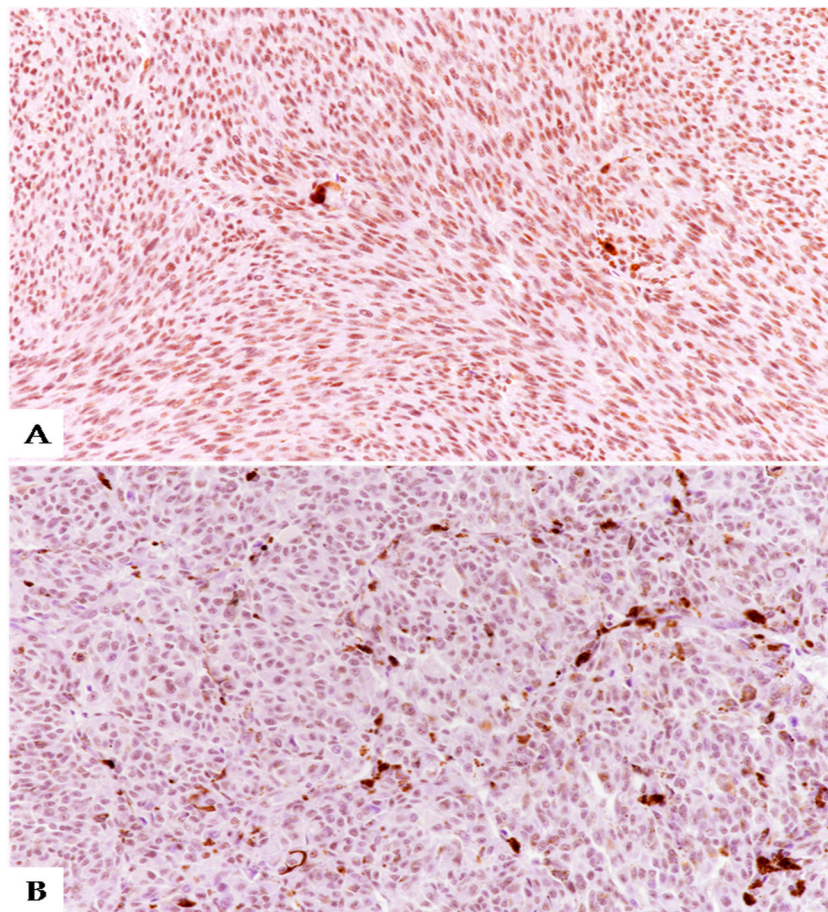
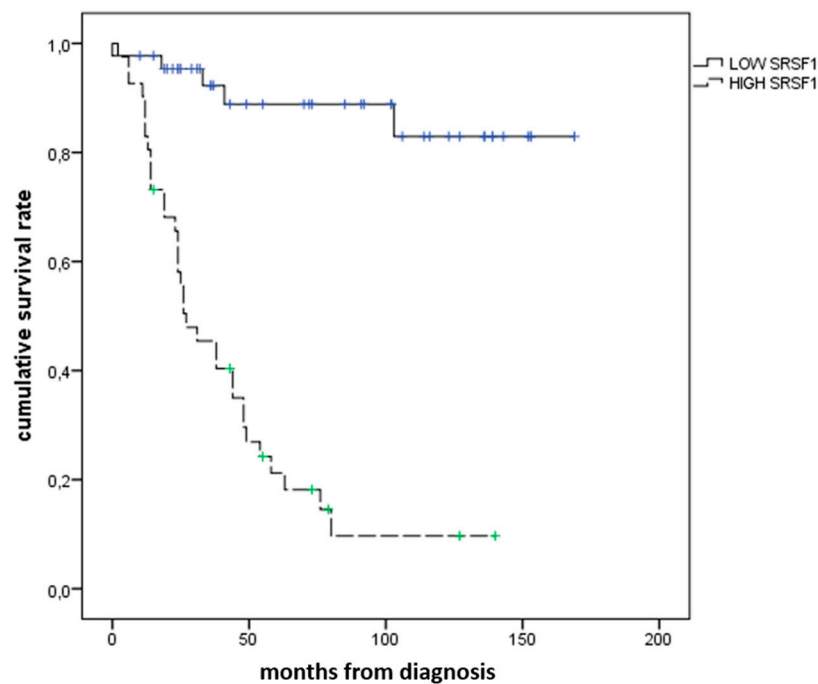


**Figure 1.** (A) Strong and diffuse immunohistochemical expression of SRSF1 in a case of spindle cell-type uveal melanoma (immunoperoxidase; original magnification 150 $\times$ ); (B) Low immunoeexpression of SRSF1 in a case of epithelioid cell-type uveal melanoma (immunoperoxidase; original magnification 150 $\times$ ).

**Table 4.** Number of uveal melanoma (with and without metastasis) with low and high SRSF1 expression and MVD (n/mm<sup>2</sup>).

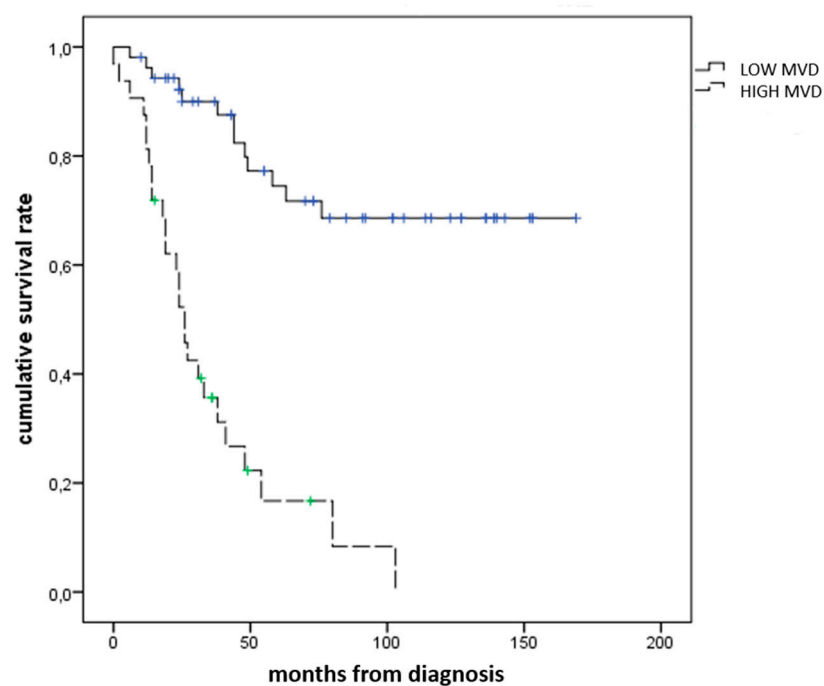
|                                | SRSF1      |                   | MVD (n/mm <sup>2</sup> ) |                    |
|--------------------------------|------------|-------------------|--------------------------|--------------------|
|                                | Low (<3)   | High ( $\geq 3$ ) | Low (<43)                | High ( $\geq 43$ ) |
| Metastasis free (n = 46)       | 39 (84.8%) | 7 (15.2%)         | 40 (87.0%)               | 6 (13.0%)          |
| Metastasis (n = 39)            | 5 (12.8%)  | 34 (87.2%)        | 13 (33.3%)               | 26 (66.7%)         |
| <i>p</i> (Fisher's exact test) | <0.001     |                   | <0.001                   |                    |

Figure 2 shows the results of the Kaplan–Meier survival analyses in UM patients with low and high SRSF1 immunoeexpression. The mean metastasis-free survival times (SE, with 95% CI) estimated were 149.1 (8.3) (CI: 132.9 to 165.3) and 43.1 (6.3) (CI: 30.1 to 55.5); a significant difference ( $p < 0.001$ ) between the two groups was found by the log-rank test.



**Figure 2.** Kaplan–Meier survival curves in patients affected by uveal melanoma with low and high SRSF1 immunohistochemical expression.

Figure 3 shows the results of Kaplan–Meier survival analyses in patients with uveal melanomas with low and high MVD expression. The mean survival time free from metastasis (SE, with 95% CI) estimated were respectively: 129.0 (9.3) (CI: 110.7 to 147.3) and 35.5 (5.6) (CI: 24.4 to 46.6). The log-rank test exhibited a significant difference ( $p < 0.001$ ) between the two groups.



**Figure 3.** Kaplan–Meier survival curves in patients affected by uveal melanoma with low and high MVD.

The above-mentioned results highly suggest a negative prognostic role for SRSF1 in UM patients. Higher expression levels of this protein are significantly associated with other poor prognostic indicators, such as epithelioid cell type and higher MVD; the latter might lead us to hypothesize a positive correlation between SRSF1 and increased tumor angiogenesis. Furthermore, as shown in Kaplan–Meier curves, we found a significant association between SRSF1, MVD and lower metastasis-free survival times in our cohort.

#### 4. Discussion

The search for novel potential reliable prognostic factors is one of the most significant objectives of cancer research in the field of UM, as it allows a stratification of patients into two large groups: those with higher risk and those with lower risk of developing distant metastases [10,29]. The absence of standardized guidelines on the exact times after which control tests should be performed and the type of tests that should be done during follow-up time makes this topic of extreme practical significance. The potential identification of a high-risk group of patients could allow the performance of more frequent controls in order to earlier diagnose cases with liver metastases that could be safely surgically excised [30]. Accordingly, in the last decade our research group reported some novel potential immunohistochemical factors with prognostic impact [5,31–35], which may be included into the list of the classically reported markers of UM, such as tumor location, tumor size, extraocular invasion, cell type, pathological T stage and immunohistochemical staining with BAP1 [14]. Recently, Luo et al. identified a ten-gene signature (SIRT3, HMCES, SLC44A3, TCTN1, STPG1, POMGNT2, RNF208, ANXA2P2, ULBP1 and CA12), able to better stratify the outcome of UM patients [36]; in detail, ANXA2P2, ULBP1, CA12 had a poor prognostic role, while the other genes a positive one. It has been also hypothesized that conventional and alternative splicing events were correlated to the overall survival of patients with cutaneous and uveal melanoma [37]. In this regard, Furney et al. found recurrent mutations of the splicing factor SF3B1 in 3/12 cases from their cohort and in 15/105 cases from an extension cohort [38]; these authors demonstrated that SF3B1 mutations were linked to differential alternative splicing of ABCC5 and UQCC genes and correlated to better outcome and lower rate of BAP1 mutations in UM [38].

SRSF1 is an RNA-binding protein with proto-oncogenic function, being involved in angiogenesis, cell migration and tumor proliferation of several types of human neoplasms, including gliomas, malignant mesotheliomas, and breast, colorectal and prostate cancers [18,20–25]. SRSF1 immunoexpression was positively associated with worse outcome, androgen-receptor status and Ki-67 proliferation rate in prostatic adenocarcinoma [27]; a significant correlation between SRSF1, MVD and shorter overall survival times was also found in fluoro-edenite-induced malignant mesothelioma [26]. In the present paper we provided the first immunohistochemical evidence of the poor prognostic role of this protein in UM; in more detail, we found a statistically significant correlation between higher SRSF1 immunohistochemical expression, higher MVD levels and poorer prognosis in terms of metastatic spread and lower metastasis-free-survival in UM. Regarding the relationship between SRSF1 and MVD, previous studies demonstrated that SRSF1 had a stimulatory function on tumor angiogenesis, resulting in a switch in the pro-angiogenic/anti-angiogenic ratio of VEGFA [17–21]; in this regard, Barbagallo et al. first reported the complex relationship between circSMARCA5, a specific subtype of circRNAs with a tumor-suppressor role, and SRSF1, demonstrating that the downregulation of circSMARCA5 along with the concomitant upregulation of SRSF1 led to increased cell migration and angiogenesis in human glioblastoma tissue and cell lines [17–19]. The MVD count, despite not representing the best method to evaluate tumor angiogenesis, is a semi-quantitative “surrogate” of this process [27]; accordingly, the positive correlation found in our cohort between SRSF1 and MVD led us to hypothesize that SRSF1 has a pro-angiogenic role also in UM.

## 5. Conclusions

Our results indicate a poor prognostic role of SRSF1 in UM, as higher immunohistochemical expression of this protein was associated with a higher risk of metastases and lower metastasis-free survival times; conversely, the cases from our cohort that exhibited lower SRSF1 levels showed both lower metastatic risk and longer metastasis-free survival. However, further multi-institutional studies on larger series are required to validate our findings and to better clarify the complex interaction between SRSF1, risk of metastasis and angiogenic potential of UM. Additional perspectives of our study also include the possibility to evaluate the immunohistochemical expression of SRSF1 as a diagnostic marker in the differential diagnosis between cutaneous melanoma and UM metastases when the primary neoplasm is unknown or in patients with two concomitant melanomas.

**Author Contributions:** Conceptualization, G.B., L.P. and R.C.; Data curation, G.B., A.L. and S.S.; Formal analysis, G.B., M.F. and P.V.F.; Investigation, A.R., M.R., A.L. and T.A.; Methodology, L.F., R.D.P. and M.L.; Resources, D.R., R.M.D.C. and S.S.; Supervision, S.S. and R.C.; Validation, L.F.; Writing—original draft, G.B. and R.C.; Writing—review & editing, G.B. and R.C. All authors have read and agreed to the published version of the manuscript.

**Funding:** This research received no external funding.

**Institutional Review Board Statement:** The present research complied with the Helsinki Declaration and all experiments were approved by the local Ethics Committee, Comitato Etico Catania 1, University of Catania (ID: 003186-24).

**Informed Consent Statement:** Not applicable.

**Data Availability Statement:** The data presented in this study are available on request from the corresponding author.

**Conflicts of Interest:** The authors declare no conflict of interest.

## References

1. Foti, P.V.; Travali, M.; Farina, R.; Palmucci, S.; Spatola, C.; Raffaele, L.; Salamone, V.; Caltabiano, R.; Broggi, G.; Puzzo, L.; et al. Diagnostic methods and therapeutic options of uveal melanoma with emphasis on MR imaging—Part I: MR imaging with pathologic correlation and technical considerations. *Insights Imaging* **2021**, *12*, 1–27. [[CrossRef](#)]
2. Foti, P.V.; Travali, M.; Farina, R.; Palmucci, S.; Spatola, C.; Liardo, R.L.E.; Milazzotto, R.; Raffaele, L.; Salamone, V.; Caltabiano, R.; et al. Diagnostic methods and therapeutic options of uveal melanoma with emphasis on MR imaging—Part II: Treatment indications and complications. *Insights Imaging* **2021**, *12*, 1–24. [[CrossRef](#)]
3. Millodot, M.; Hendler, K.; Pe'Er, J. Iris melanoma: A case report and review. *Ophthalmic Physiol. Opt.* **2006**, *26*, 120–126. [[CrossRef](#)] [[PubMed](#)]
4. Fallico, M.; Raciti, G.; Longo, A.; Reibaldi, M.; Bonfiglio, V.; Russo, A.; Caltabiano, R.; Gattuso, G.; Falzone, L.; Avitabile, T. Current molecular and clinical insights into uveal melanoma (Review). *Int. J. Oncol.* **2021**, *58*, 10. [[CrossRef](#)]
5. Broggi, G.; Musumeci, G.; Puzzo, L.; Russo, A.; Reibaldi, M.; Ragusa, M.; Longo, A.; Caltabiano, R. Immunohistochemical Expression of ABCB5 as a Potential Prognostic Factor in Uveal Melanoma. *Appl. Sci.* **2019**, *9*, 1316. [[CrossRef](#)]
6. Kaliki, S.; Shields, C.L. Uveal melanoma: Relatively rare but deadly cancer. *Eye* **2016**, *31*, 241–257. [[CrossRef](#)]
7. Kaliki, S.; Shields, C.L.; Shields, J.A. Uveal melanoma: Estimating prognosis. *Indian J. Ophthalmol.* **2015**, *63*, 93–102. [[CrossRef](#)]
8. Foti, P.; Inì, C.; Travali, M.; Farina, R.; Palmucci, S.; Spatola, C.; Liardo, R.; Milazzotto, R.; Raffaele, L.; Salamone, V.; et al. MR Imaging—Pathologic Correlation of Uveal Melanomas Undergoing Secondary Enucleation after Proton Beam Radiotherapy. *Appl. Sci.* **2021**, *11*, 4310. [[CrossRef](#)]
9. Milam, R.W.; Batson, S.A.; Breazzano, M.P.; Ayala-Peacock, D.N.; Daniels, A.B. Modern and Novel Radiotherapy Approaches for the Treatment of Uveal Melanoma. *Int. Ophthalmol. Clin.* **2017**, *57*, 11–27. [[CrossRef](#)]
10. Broggi, G.; Salvatorelli, L. Bio-Pathological Markers in the Diagnosis and Therapy of Cancer. *Cancers* **2020**, *12*, 3113. [[CrossRef](#)]
11. Falzone, L.; Romano, G.L.; Salemi, R.; Bucolo, C.; Tomasello, B.; Lupo, G.; Anfusio, C.D.; Spandidos, D.; Libra, M.; Candido, S. Prognostic significance of deregulated microRNAs in uveal melanomas. *Mol. Med. Rep.* **2019**, *19*, 2599–2610. [[CrossRef](#)]
12. Stålhammar, G.; Grossniklaus, H. Intratumor Heterogeneity in Uveal Melanoma BAP-1 Expression. *Cancers* **2021**, *13*, 1143. [[CrossRef](#)]
13. Stålhammar, G.; See, T.R.O.; Phillips, S.; Seregard, S.; Grossniklaus, H.E. Digital Image Analysis of BAP-1 Accurately Predicts Uveal Melanoma Metastasis. *Transl. Vis. Sci. Technol.* **2019**, *8*, 11. [[CrossRef](#)]
14. Broggi, G.; Russo, A.; Reibaldi, M.; Russo, D.; Varricchio, S.; Bonfiglio, V.; Spatola, C.; Barbagallo, C.; Foti, P.V.; Avitabile, T.; et al. Histopathology and Genetic Biomarkers of Choroidal Melanoma. *Appl. Sci.* **2020**, *10*, 8081. [[CrossRef](#)]

15. Zhou, X.; Wang, R.; Li, X.; Yu, L.; Hua, D.; Sun, C.; Shi, C.; Luo, W.; Rao, C.; Jiang, Z.; et al. Splicing factor SRSF1 promotes gliomagenesis via oncogenic splice-switching of MYO1B. *J. Clin. Investig.* **2019**, *129*, 676–693. [[CrossRef](#)] [[PubMed](#)]
16. Zhou, X.; Li, X.; Yu, L.; Wang, R.; Hua, D.; Shi, C.; Sun, C.; Luo, W.; Rao, C.; Jiang, Z.; et al. The RNA-binding protein SRSF1 is a key cell cycle regulator via stabilizing NEAT1 in glioma. *Int. J. Biochem. Cell Biol.* **2019**, *113*, 75–86. [[CrossRef](#)]
17. Barbagallo, D.; Caponnetto, A.; Cirnigliaro, M.; Brex, D.; Barbagallo, C.; D'Angeli, F.; Morrone, A.; Caltabiano, R.; Barbagallo, G.M.; Ragusa, M.; et al. CircSMARCA5 Inhibits Migration of Glioblastoma Multiforme Cells by Regulating a Molecular Axis Involving Splicing Factors SRSF1/SRSF3/PTB. *Int. J. Mol. Sci.* **2018**, *19*, 480. [[CrossRef](#)] [[PubMed](#)]
18. Barbagallo, D.; Caponnetto, A.; Brex, D.; Mirabella, F.; Barbagallo, C.; Lauretta, G.; Morrone, A.; Certo, F.; Broggi, G.; Caltabiano, R.; et al. CircSMARCA5 Regulates VEGFA mRNA Splicing and Angiogenesis in Glioblastoma Multiforme Through the Binding of SRSF1. *Cancers* **2019**, *11*, 194. [[CrossRef](#)] [[PubMed](#)]
19. Barbagallo, D.; Caponnetto, A.; Barbagallo, C.; Battaglia, R.; Mirabella, F.; Brex, D.; Stella, M.; Broggi, G.; Altieri, R.; Certo, F.; et al. The GAUGAA Motif Is Responsible for the Binding between circSMARCA5 and SRSF1 and Related Downstream Effects on Glioblastoma Multiforme Cell Migration and Angiogenic Potential. *Int. J. Mol. Sci.* **2021**, *22*, 1678. [[CrossRef](#)]
20. Broggi, G.; Salvatorelli, L.; Barbagallo, D.; Certo, F.; Altieri, R.; Tirrò, E.; Massimino, M.; Vigneri, P.; Guadagno, E.; Maugeri, G.; et al. Diagnostic Utility of the Immunohistochemical Expression of Serine and Arginine Rich Splicing Factor 1 (SRSF1) in the Differential Diagnosis of Adult Gliomas. *Cancers* **2021**, *13*, 2086. [[CrossRef](#)]
21. Stella, M.; Falzone, L.; Caponnetto, A.; Gattuso, G.; Barbagallo, C.; Battaglia, R.; Mirabella, F.; Broggi, G.; Altieri, R.; Certo, F.; et al. Serum Extracellular Vesicle-Derived circHIPK3 and circSMARCA5 Are Two Novel Diagnostic Biomarkers for Glioblastoma Multiforme. *Pharmaceuticals* **2021**, *14*, 618. [[CrossRef](#)] [[PubMed](#)]
22. Anczukow, O.; Akerman, M.; Cléry, A.; Wu, J.; Shen, C.; Shirole, N.H.; Raimer, A.; Sun, S.; Jensen, M.A.; Hua, Y.; et al. SRSF1-Regulated Alternative Splicing in Breast Cancer. *Mol. Cell* **2015**, *60*, 105–117. [[CrossRef](#)]
23. Sheng, J.; Zhao, Q.; Zhao, J.; Zhang, W.; Sun, Y.; Qin, P.; Lv, Y.; Bai, L.; Yang, Q.; Chen, L.; et al. SRSF1 modulates PTPMT1 alternative splicing to regulate lung cancer cell radioresistance. *EBioMedicine* **2018**, *38*, 113–126. [[CrossRef](#)] [[PubMed](#)]
24. Malakar, P.; Shilo, A.; Mogilevsky, A.; Stein, I.; Pikarsky, E.; Nevo, Y.; Benyamini, H.; Elgavish, S.; Zong, X.; Prasanth, K.V.; et al. Long Noncoding RNA MALAT1 Promotes Hepatocellular Carcinoma Development by SRSF1 Upregulation and mTOR Activation. *Cancer Res.* **2016**, *77*, 1155–1167. [[CrossRef](#)]
25. Li, H.; Guo, S.; Zhang, M.; Li, L.; Wang, F.; Song, B. Long non-coding RNA AGAP2-AS1 accelerates cell proliferation, migration, invasion and the EMT process in colorectal cancer via regulating the miR-4,668-3p/SRSF1 axis. *J. Gene Med.* **2020**, *22*, e3250. [[CrossRef](#)] [[PubMed](#)]
26. Broggi, G.; Angelico, G.; Filetti, V.; Ledda, C.; Lombardo, C.; Vitale, E.; Rapisarda, V.; Loreto, C.; Caltabiano, R. Immunohistochemical Expression of Serine and Arginine-Rich Splicing Factor 1 (SRSF1) in Fluoro-Edenite-Induced Malignant Mesothelioma: A Preliminary Study. *Int. J. Environ. Res. Public Health* **2021**, *18*, 6249. [[CrossRef](#)]
27. Broggi, G.; Giudice, A.L.; Di Mauro, M.; Asmundo, M.G.; Pricoco, E.; Piombino, E.; Caltabiano, R.; Morgia, G.; Russo, G.I. SRSF-1 and microvessel density immunohistochemical analysis by semi-automated tissue microarray in prostate cancer patients with diabetes (DIAMOND study). *Prostate* **2021**, *81*, 882–892. [[CrossRef](#)]
28. Broggi, G.; Filetti, V.; Ieni, A.; Rapisarda, V.; Ledda, C.; Vitale, E.; Varricchio, S.; Russo, D.; Lombardo, C.; Tuccari, G.; et al. MacroH2A1 Immunoexpression in Breast Cancer. *Front. Oncol.* **2020**, *10*, 1519. [[CrossRef](#)]
29. Gajdzis, M.; Kaczmarek, R.; Gajdzis, P. Novel Prognostic Immunohistochemical Markers in Uveal Melanoma-Literature Review. *Cancers* **2021**, *13*, 4031. [[CrossRef](#)]
30. Agarwala, S.S.; Eggermont, A.M.M.; O'Day, S.; Zager, J.S. Metastatic melanoma to the liver: A contemporary and comprehensive review of surgical, systemic, and regional therapeutic options. *Cancer* **2013**, *120*, 781–789. [[CrossRef](#)]
31. Caltabiano, R.; Puzzo, L.; Barresi, V.; Ieni, A.; Loreto, C.; Musumeci, G.; Castrogiovanni, P.; Ragusa, M.; Foti, P.; Russo, A.; et al. ADAM 10 expression in primary uveal melanoma as prognostic factor for risk of metastasis. *Pathol. Res. Pract.* **2016**, *212*, 980–987. [[CrossRef](#)]
32. Barbagallo, C.; Caltabiano, R.; Broggi, G.; Russo, A.; Puzzo, L.; Avitabile, T.; Longo, A.; Reibaldi, M.; Barbagallo, D.; Di Pietro, C.; et al. LncRNA *LINC00518* Acts as an Oncogene in Uveal Melanoma by Regulating an RNA-Based Network. *Cancers* **2020**, *12*, 3867. [[CrossRef](#)] [[PubMed](#)]
33. Salvatorelli, L.; Puzzo, L.; Russo, A.; Reibaldi, M.; Longo, A.; Ragusa, M.; Aldo, C.; Rappazzo, G.; Caltabiano, R.; Salemi, M. Immunoexpression of SPANX-C in metastatic uveal melanoma. *Pathol. Res. Pract.* **2019**, *215*, 152431. [[CrossRef](#)]
34. Russo, D.; Di Crescenzo, R.M.; Broggi, G.; Merolla, F.; Martino, F.; Varricchio, S.; Ilardi, G.; Borzillo, A.; Carandente, R.; Pignatiello, S.; et al. Expression of P16INK4a in Uveal Melanoma: New Perspectives. *Front. Oncol.* **2020**, *10*, 562074. [[CrossRef](#)]
35. Broggi, G.; Ieni, A.; Russo, D.; Varricchio, S.; Puzzo, L.; Russo, A.; Reibaldi, M.; Longo, A.; Tuccari, G.; Staibano, S.; et al. The Macro-Autophagy-Related Protein Beclin-1 Immunohistochemical Expression Correlates with Tumor Cell Type and Clinical Behavior of Uveal Melanoma. *Front. Oncol.* **2020**, *10*, 589849. [[CrossRef](#)]
36. Luo, H.; Ma, C.; Shao, J.; Cao, J. Prognostic Implications of Novel Ten-Gene Signature in Uveal Melanoma. *Front. Oncol.* **2020**, *10*, 567512. [[CrossRef](#)] [[PubMed](#)]

- 
37. Ma, F.; He, R.; Lin, P.; Zhong, J.; Ma, J.; Yang, H.; Hu, X.; Chen, G. Profiling of prognostic alternative splicing in melanoma. *Oncol. Lett.* **2019**, *18*, 1081–1088. [[CrossRef](#)] [[PubMed](#)]
  38. Furney, S.; Pedersen, M.; Gentien, D.; Dumont, A.G.; Rapinat, A.; Desjardins, L.; Turajlic, S.; Piperno-Neumann, S.; De La Grange, P.; Roman-Roman, S.; et al. SF3B1 Mutations Are Associated with Alternative Splicing in Uveal Melanoma. *Cancer Discov.* **2013**, *3*, 1122–1129. [[CrossRef](#)]